Three-body parameter for Efimov states in ⁶Li

Bo Huang (黄博),[1] Kenneth M. O'Hara,[2,3] Rudolf Grimm,[1,3] Jeremy M. Hutson,[4] and Dmitry S. Petrov[5]

[1]*Institut für Experimentalphysik, Universität Innsbruck, 6020 Innsbruck, Austria*
[2]*Department of Physics, Pennsylvania State University, University Park, Pennsylvania 16802-6300, USA*
[3]*Institut für Quantenoptik und Quanteninformation (IQOQI), Österreichische Akademie der Wissenschaften, 6020 Innsbruck, Austria*
[4]*Joint Quantum Centre (JQC) Durham/Newcastle, Department of Chemistry, Durham University, South Road,
Durham, DH1 3LE, United Kingdom*
[5]*Université Paris-Sud, CNRS, LPTMS, UMR8626, Orsay F-91405, France*

We present a state-of-the-art reanalysis of experimental results on Efimov resonances in the three-fermion system of ⁶Li. We discuss different definitions of the three-body parameter (3BP) for Efimov states and adopt a definition that excludes effects due to deviations from universal scaling for low-lying states. We develop a finite-temperature model for the case of three distinguishable fermions and apply it to the excited-state Efimov resonance to obtain the most accurate determination to date of the 3BP in an atomic three-body system. Our analysis of ground-state Efimov resonances in the same system yields values for the three-body parameter that are consistent with the excited-state result. Recent work has suggested that the reduced 3BP for atomic systems is a near-universal quantity, almost independent of the particular atom involved. However, the value of the 3BP obtained for ⁶Li is significantly (∼20%) different from that previously obtained from the excited-state resonance in Cs. The difference between these values poses a challenge for theory.

I. INTRODUCTION

Ultracold atomic gases with resonant interactions provide experimental model systems to explore the universal physics of few-body quantum states [1,2]. Efimov states, which are weakly bound three-body quantum states in systems of resonantly interacting particles, are a paradigm of this field. Efimov [3] showed that, when two bosons interact with an infinite scattering length, the corresponding three-particle system has an infinite number of three-body states just below threshold. For zero-range interactions, each successive Efimov state is larger than the previous one by a discrete length scaling factor, the "Efimov period," which is 22.7 for a system of three identical bosons [4] but can be widely different for other systems [5]. We refer to this universal scaling behavior as Efimov universality.

The interactions between pairs of ultracold atoms may be varied by tuning an applied magnetic field in the vicinity of a zero-energy Feshbach resonance [6]. The scattering length has a pole at resonance, corresponding to a two-body bound state exactly at threshold. Signatures of Efimov states were first observed in an ultracold gas of cesium atoms [7] and have since been found in many other systems, including other bosonic gases [8–13], three-component fermionic spin mixtures [14–17], and mixtures of atomic species [18–21]. Moreover, extensions of the Efimov scenario to universal states of larger clusters [22–24] have been demonstrated in experiments [9,25,26], highlighting the general nature of universal few-body physics.

In addition to their discrete scaling property, Efimov states are characterized by a *three-body parameter* (3BP), which determines the position of the entire ladder of states. In the realm of nuclear systems, the 3BP is a nonuniversal quantity [1], determined by details of the short-range interaction. However, in atomic systems it has been found experimentally [13,27] that the 3BP is nearly constant when expressed in terms

of the van der Waals length r_{vdW} [6], which quantifies the dispersion interaction between two neutral atoms. We refer to this feature of Efimov physics as van der Waals universality of the 3BP, and it has been the subject of a number of theoretical investigations [28–33].

Three-body recombination resonances occur when Efimov states cross the three-atom threshold as a function of magnetic field (and hence of scattering length) [34–36]. Recombination resonances due to Efimov ground states provide the most prominent observables in Efimov physics. Many experiments have focused on such features, including some that determined the 3BP [12,13,27]. In real atomic systems, however, finite-range corrections may significantly affect universal scaling, particularly for ratios involving the Efimov ground state [30,37–39]. However, such corrections decrease substantially for higher Efimov states and are already very small for the first excited state. Excited-state resonances are therefore particularly interesting for precise measurements of the 3BP.

Excited-state Efimov resonances occur at very large scattering lengths. They require extremely low temperatures for experimental observation since the recombination peaks are less well defined when the de Broglie wavelengths are shorter than the scattering lengths [7,40,41]. Excited-state resonances have therefore been observed in only a very few experiments carried out with ⁶Li [16], with ¹³³Cs [42], and with mixtures of ⁶Li and ¹³³Cs [20,21]. Quantitative understanding of these resonances requires both very precise knowledge of the two-body scattering properties and an accurate theoretical description of finite-temperature effects. Reference [42] analyzed the excited-state Efimov resonance in cesium using a highly accurate model of the two-body scattering [43] and a theoretical finite-temperature approach recently developed in Ref. [41]. This study provided the most precise measurement of the Efimov period so far.

In this article, we reanalyze previous experimental results on the excited-state Efimov resonance in ^{6}Li observed in Ref. [16] and on the ground-state Efimov resonances observed in Refs. [14] and [15]. In Sec. II, we discuss different definitions of the 3BP and how they are affected by deviations from ideal Efimov behavior. We adopt a definition that excludes effects due to deviations from universal scaling for low-lying states. In Sec. III, we summarize the main properties of the three-fermion system. In Sec. IV, we develop a new finite-temperature approach which generalizes the theory introduced for the three-boson case in Ref. [41] to the case of three distinguishable fermions. In Sec. V, we present a refined analysis of the excited-state resonance observed in Ref. [16]. This gives a high-precision value for the 3BP in ^{6}Li, which deviates significantly from those found in other atomic systems. In Sec. VI, we reanalyze previous results on the ground-state Efimov resonance from Ref. [14] and investigate the possible influence of finite-range effects. In Sec. VII, we discuss our findings in the context of other experiments in the field. The value of the 3BP found for ^{6}Li is not well explained by current theories and presents a challenge for future theoretical work.

II. THREE-BODY PARAMETER

For three identical bosons, ideal Efimov scaling leads to the simple relation

$$\kappa^{(n+1)} = \kappa^{(n)}/22.7 \tag{1}$$

between the wave numbers $\kappa^{(n)}$ that characterize the energies $E_{res}^{(n)} = -(\hbar\kappa^{(n)})^2/m$ of successive Efimov states in the resonant limit $a \to \pm\infty$. Here m is the atomic mass, and n is an integer quantum number. The corresponding relation between the scattering lengths at the positions of successive recombination resonances is

$$a_-^{(n+1)} = 22.7 a_-^{(n)}. \tag{2}$$

The universal relation

$$a_-^{(n)} = -1.508/\kappa^{(n)} \tag{3}$$

connects a resonance position with the corresponding bound-state wave number. In the ideal case, knowledge of any of the above quantities $\kappa^{(n)}$ or $a_-^{(n)}$ fixes the infinite series and thus provides a proper representation of the 3BP.

In a real system, where the interaction has a finite range, the Efimov spectrum is bounded from below. We refer to the lowest state as the Efimov ground state with $n = 0$ and to the corresponding resonance at $a_-^{(0)}$ as the ground-state Efimov resonance. Equations (1)–(3) then represent approximations, subject to finite-range effects.

One way to understand the Efimov effect is through a treatment in hyperspherical coordinates. Efimov states may be considered to be supported by an effective adiabatic potential that is a function of the hyperradius R. For a zero-range two-body potential with large scattering length a, this potential is attractive and proportional to R^{-2} for $R \lesssim |a|$ [44] and supports an infinite number of bound states as $a \to \pm\infty$. For potential curves with long-range van der Waals tails, however, Wang *et al.* [29] have shown that the effective adiabatic potential reaches a minimum and then rises to a wall or

barrier near $R = 2r_{\text{vdW}}$. The positions of the minimum and wall depend to some extent on the details of the two-body potential and the number of bound states it supports but become nearly universal as the number of two-body bound states increases. The presence of the minimum and wall has two principal effects on the physics. First, the deviation of the effective potential from R^{-2} behavior results in deviations from ideal Efimov scaling for the lowest-lying states. Second, the boundary condition provided by the wall defines the position of the entire ladder of Efimov states, and its nearly universal position is responsible for the near universality of the 3BP. However, it should be noted that the wall itself is a product of physics around $2r_{\text{vdW}}$, so that variations in the physics in this region can produce deviations from the universality of the 3BP even in the limit $a \to \pm\infty$.

Theoretical investigations [29,30,37,38] have shown that the Efimov ground state may be subject to considerable modifications. For $n = 0$ this may change the factor 22.7 in Eqs. (1)–(2) by up to 25%. Relation (3) is subject to similar modifications [29,30]. The recent experiment on the excited-state resonance in Cs [42] and a related theoretical investigation [33] also hint at deviations from the ideal scaling.

The deviations from universal scaling for low-lying Efimov states raise the question of the best representation of the 3BP. Definitions based on the limit $n \to \infty$ remove effects of this type from the 3BP. Accordingly, we adopt the definition [1]

$$\kappa_* = \lim_{n\to\infty} (22.7^n \kappa^{(n)}), \tag{4}$$

and by analogy

$$a_-^* = \lim_{n\to\infty} \frac{a_-^{(n)}}{22.7^n}. \tag{5}$$

The position of the ground-state Efimov resonance, $a_-^{(0)}$, is commonly used as a 3BP. However, it gives a somewhat crude approximation to a_-^* and, in some cases, may deviate from it by as much as 25%. The quantities $a_-^{(1)}/22.7$ and $22.7\kappa^{(1)}$, obtained from the excited-state resonance, provide much better approximations to a_-^* and κ_*, with corrections of only about 1% due to deviations from universal scaling [30]; these corrections are comparable to the other uncertainties in current experiments.

Efimov states are also characterized by a decay parameter η_* [1], which describes their decay to lower-lying atom-dimer combinations. This parameter is usually considered to be a constant for a particular Efimov state but may vary if the available product states change significantly. The resulting field dependence may be important when interpreting measurements that extend over wide ranges of field [45].

III. EFIMOV STATES IN A THREE-COMPONENT FERMI GAS

A. Three-fermion system

Efimov states in a three-component gas of fermions [46] exhibit the same discrete scaling behavior as in the three-boson case, provided that all three scattering lengths involved are large ($|a_{12}|, |a_{13}|, |a_{23}| \gg r_{\text{vdW}}$). In particular, if the masses of the three components are equal, the Efimov period is given by the same discrete scaling factor of 22.7 [4]. The special case

of three equal scattering lengths ($a_{12} = a_{13} = a_{23}$) is formally equivalent to the situation for three identical bosons.

A gas of ^{6}Li atoms prepared in a mixture of the lowest three spin states allows a realization of large scattering lengths by Feshbach tuning [6]. However, the applied magnetic field offers only one degree of freedom for tuning, thus limiting the experimentally accessible combinations of scattering lengths. Arbitrary combinations and, in particular, the situation of three equal scattering lengths thus remain hypothetical cases, but universal theory allows them to be linked to the combinations that exist in real systems.

In real experiments on a three-fermion system, Efimov resonances appear at certain combinations of large scattering lengths a_{12}, a_{13}, a_{23}, where typically $a_{12} \neq a_{13} \neq a_{23}$. A generalization of the Skorniakov–Ter-Martirosian (STM) equations [46] can be employed to determine the 3BP from these generally unequal values. In the wave number representation, κ_* then refers to the hypothetical case of three infinite scattering lengths, while a_-^* refers to a hypothetical system with three equal scattering lengths.

The STM approach is based on the zero-range approximation and therefore does not take into account finite-range corrections, which are significant at relatively small scattering lengths. It can thus be expected to provide an excellent approximation for excited Efimov states ($n \geqslant 1$), but it may be subject to significant corrections if applied to the Efimov ground state ($n = 0$).

B. Three-body recombination

In a three-component Fermi gas, the dominant contribution to three-body losses results from triples of three nonidentical particles. All other combinations involve pairs of identical fermions, which leads to a strong Pauli suppression of losses at ultralow temperatures [47].

Three-body losses can be modeled by the simple rate equation

$$\frac{d}{dt}n_i = -L_3 n_1 n_2 n_3, \tag{6}$$

where n_i represent the number densities of the three different spin states. After a spatial integration of losses over the density profile of the trapped cloud, the loss rate coefficient L_3 can be experimentally determined by fitting the time-dependent decay of the total atom numbers [14–16]. Efimov states show up as distinct loss resonances [36] when they couple to the three-atom threshold.

C. Lithium-6

The situation of a three-component Fermi gas of ^{6}Li is unique because of overlapping Feshbach resonances in all three combinations of the lowest three spin states together with large negative background scattering lengths. The two-body scattering properties are known to an extraordinarily high level of precision thanks to the characterization in Ref. [48], which significantly improved the conversion from magnetic field to scattering lengths compared to previous work [49].

In the resonance region between 832 and 900 G, all three scattering lengths are very large and negative, with absolute values of a few thousand times the Bohr radius a_0 that vastly exceed $r_{vdW} = 31.26 a_0$. In this extreme regime, an excited Efimov state exists [16]. This trimer state crosses the three-atom threshold near 900 G and leads to a strong enhancement of three-body recombination. The corresponding Efimov ground state exists over a much wider range of magnetic fields, but it does not cross the threshold at currently accessible magnetic fields and thus does not lead to an observable recombination resonance.

In the magnetic-field region below the zero crossings of the Feshbach resonances, the three scattering lengths are moderately large and negative, so that an Efimov ground state exists. This state crosses the three-atom threshold near 130 G and near 500 G [14,15], leading to two observable Efimov resonances. In this low-field region, the scattering lengths never reach large enough values for an excited Efimov state to exist.

D. The effective range

One way to quantify the finite (nonzero) range of an atomic interaction is through the effective range [50,51], which characterizes the leading term in the energy dependence of the scattering length. The effective range behaves very differently in the vicinity of Feshbach resonances of different types [52]. For a resonance that is strongly entrance-channel-dominated [6], the effective range takes a small and fairly constant value close to $2.8 r_{vdW}$ at fields near the resonance pole [53]. By contrast, for resonances that are closed-channel-dominated, the effective range is much larger and varies very fast with magnetic field [52]. The Feshbach resonances used in the present work for ^{6}Li are all strongly entrance channel dominated [6], so that deviations from Efimov scaling due to finite-range effects are expected to be relatively small in comparison to some of the other atomic systems that have been studied.

IV. FINITE-TEMPERATURE THEORETICAL APPROACH

A convenient way of modeling three-body losses in Efimovian systems is provided by the S-matrix formalism based on Efimov's radial law [54], which is elaborated in Refs. [1,41,55] for the case of three identical bosons. Its generalization to three distinguishable atoms with different scattering lengths is straightforward, and we will present only a brief derivation. This is a zero-range theory for which κ_* and η_* are external parameters.

First, one introduces three-atom scattering channels describing the motion of free atoms at large distances. By contrast, all atom-dimer channels are substituted by the single Efimov channel defined in the scaling region $r_{vdW} \ll R \ll \min\{1/k, |a_{12}|, |a_{23}|, |a_{13}|\}$, where $k = \sqrt{mE}/\hbar$, E is the energy in the center-of-mass reference frame, R is the hyperradius, and we consider the case of negative scattering lengths. The reason for this substitution is that, when $r_{vdW} \ll \min\{1/k, |a_{12}|, |a_{23}|, |a_{13}|\}$, this channel becomes essentially the only one that can conduct three atoms from large distances to the recombination region of size $\sim r_{vdW}$.

One can think of this short-distance channel and the long-distance three-atom channels as being fused together at intermediate distances where the transmission, reflection, and

mixing of the channels takes place. We can then introduce a unitary matrix s_{ij}, which defines the amplitude of the outgoing wave in channel j if the incoming wave is injected in channel i. The terms "incoming" and "outgoing" are defined with respect to the fusion region. In particular, the incoming Efimov wave R^{-2+is_0} actually propagates towards larger distances, and R^{-2-is_0} describes the outgoing one. Here $s_0 \approx 1.00624$ is a constant, and the ideal Efimov period of 22.7 is e^{π/s_0}.

The simple fact that the matrix s_{ij} is unitary turns out to be very useful in describing the scaling properties of Efimovian systems [1]. We point out that s_{ij} does not depend on the 3BP κ_* or the decay parameter η_*. These quantities come into play when one fixes the relative phase and amplitude of the incoming and outgoing Efimov waves,

$$R^2 \Psi \propto (R/R_0)^{is_0} - e^{2\eta_*}(R/R_0)^{-is_0}, \quad (7)$$

where R_0 is a three-body length related to κ_* by

$$(\kappa_* R_0/2)^{2is_0} = -\Gamma(is_0)/\Gamma(-is_0) \quad (8)$$

and Γ is the gamma function. One can imagine that Efimov waves are reflected at small hyperradii by a lossy mirror with reflection and loss properties given by Eq. (7). The three-body problem is then analogous to a Fabry-Pérot interferometer with the other mirror quantified by the matrix s_{ij}. This picture gives a convenient way of understanding and describing three-body loss peaks as resonances of the Fabry-Pérot cavity. In particular, if we denote the Efimov channel by a subscript 1, the loss probability for a given incoming channel $i \neq 1$ is [55]

$$P_i = \frac{(1 - e^{-4\eta_*})|s_{i1}|^2}{|1 + (kR_0)^{-2is_0}e^{-2\eta_*}s_{11}|^2}, \quad (9)$$

where the denominator accounts for multiple reflections "inside" the resonator. The total loss rate constant for three distinguishable fermions is obtained by using unitarity ($\sum_{i=1}^{\infty} |s_{1i}|^2 = 1$) and averaging over the Boltzmann distribution,

$$L_3 = \frac{24\sqrt{3}\pi^2\hbar(1 - e^{-4\eta_*})}{mk_{\mathrm{th}}^6} \int_0^\infty \frac{(1 - |s_{11}|^2)e^{-k^2/k_{\mathrm{th}}^2}}{|1 + (kR_0)^{-2is_0}e^{-2\eta_*}s_{11}|^2} k\,dk, \quad (10)$$

where $k_{\mathrm{th}} = \sqrt{mk_BT}/\hbar$. Equation (10) differs from the bosonic result of Ref. [41] only by the factor $1/3$, which is due to the bosonic bunching effect and different ways of counting triples in the two cases. A more profound change is hidden in the quantity s_{11}, which, in contrast to the case of identical bosons, now depends on three dimensionless numbers, ka_{12}, ka_{23}, and ka_{13}.

In order to determine s_{11} we look for the three-body wave function that behaves as $A(kR)^{-2+is_0} + B(kR)^{-2-is_0}$ in the scaling region and contains only outgoing waves at large distances. By definition, $s_{11} = B/A$. We solve this problem by using the STM equations in a very close analogy to the bosonic case (see Supplemental Material of [41]). For distinguishable atoms with generally different scattering lengths we end up with three coupled STM equations (see Ref. [56] for details of the method).

In practice, we use the known dependence of a_{ij} on B [48] and tabulate s_{11} as a function of k and B. This then allows fast integration of Eq. (10) for any desired values of T, κ_*, and η_*.

V. EXCITED-STATE EFIMOV RESONANCE

In Ref. [16], the excited-state Efimov resonance was observed in the high-field region of ^{6}Li. In Fig. 1 we show the experimental results for the three-body loss coefficient L_3 as a function of the magnetic field, measured for two different temperatures of about 30 nK (set A) and 180 nK (set B). In this section we reanalyze these results, taking into account finite-temperature effects using the theory described in Sec. IV, in order to obtain a refined estimate of the 3BP for ^{6}Li.

The two free parameters in the temperature-dependent theory of Sec. IV are the 3BP κ_* and the decay parameter η_*. In addition, experimental uncertainties in the number density calibration may considerably affect the amplitude of the observed losses. Such uncertainties may result from the atom number calibration, from the limited knowledge of the trap frequencies, and from errors in the temperature measurements. It is therefore useful to introduce an additional scaling parameter λ for the amplitude of the observed losses [42]. Under realistic experimental conditions, variations of up to a factor of 2 from the ideal value $\lambda = 1$ are plausible.

To analyze the data we follow several different strategies, similar to those applied to the three-boson case of cesium [42]. First, we fix the temperature T to the measured values $T_{\mathrm{meas}} = 30$ nK (set A) and 180 nK (set B), and we perform a fit with κ_*, η_*, and λ as the free parameters. Alternatively, we allow for a variable temperature T, and instead, we fix $\lambda = (T/T_{\mathrm{meas}})^{-3}$ [57] to take into account the resulting change in the volume of the harmonically trapped gas. Moreover, we fit data sets A and B on either a linear or a logarithmic scale, which puts different weights on the different regions. In this way, we obtain four different fits for each data set. We note that the experimental results of Ref. [16] indicated that the effect of heating during the decay of the trapped sample remained very small, so this effect can safely be neglected in our fit analysis.
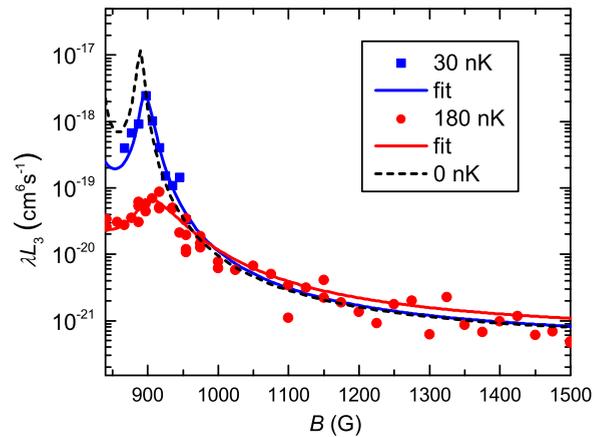

FIG. 1. (Color online) Finite-temperature fits to the excited-state Efimov resonance. The experimental results obtained for L_3 in Ref. [16] for two different temperatures are plotted as blue squares (set A, 30 nK) and red circles (set B, 180 nK). The amplitude scaling factor λ is of the order of 1, see the text. The corresponding solid lines are the fixed-temperature fits to both data sets, carried out on a linear scale (see first and fifth rows in Table I). The black dashed curve is calculated for the zero-temperature limit using the parameters from the fixed-temperature fit to the 30 nK set.

TABLE I. Results of fits for the excited-state Efimov resonance, obtained from the two sets of measurements presented in Fig. 1. The fits using a logarithmic L_3 scale are indicated by "log" in the first column.

Set	T (nK)	$\kappa_* a_0$	η_*	λ
A	30[a]	0.006 808(36)	0.032(5)	0.546(27)
A log	30[a]	0.006 744(91)	0.048(15)	0.498(107)
A	35(5)	0.006 774(39)	0.029(5)	0.644[b]
A log	36(2)	0.006 689(97)	0.042(14)	0.593[b]
B	180[a]	0.006 839(80)	0.088(15)	0.258(16)
B log	180[a]	0.006 665(130)	0.067(16)	0.270(49)
B	237(5)	0.006 736(84)	0.072(15)	0.438[b]
B log	218(10)	0.006 624(118)	0.034(8)	0.562[b]

[a]This parameter is kept fixed.
[b]This parameter is calculated from the fitted value for T.

Table I summarizes the results of our fits for both data sets, and Fig. 2 shows the values obtained for the 3BP (from the third column of Table I). The comparison between the four different fits for each data set provides information on the robustness of the fits and possible systematic effects beyond simple statistical uncertainties. In our results from the low-temperature set, set A, the errors on κ_* from individual fits range between 0.5% (for linear fits) and 1.5% (for logarithmic fits). Within the error bars no significant systematic deviations appear between the central values obtained from the different fits, which shows that the errors are consistent with purely statistical uncertainties. From the low-temperature data set (set A), by calculating a weighted average [58] over all four fitted values, we obtain the final value $\kappa_* = 0.00678(6)a_0^{-1}$, where the uncertainty includes both the weighted errors of the four individual fits and the standard deviation of the four slightly different values. The result for κ_* and the error are shown by the dashed horizontal line and the gray-shaded region in Fig. 2. Note that all the statistical uncertainties specified in this work correspond to one standard deviation.

The higher-temperature data set, set B, yields similar results, but with somewhat larger uncertainties. Again, there are no systematic deviations between the four different fit
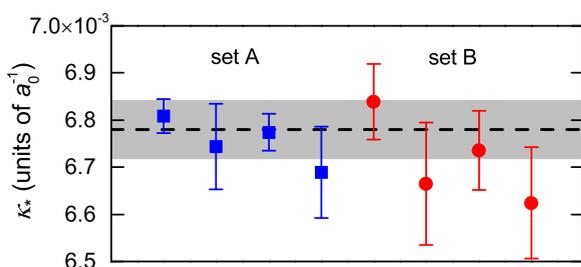

FIG. 2. (Color online) Fitted values for κ_* corresponding to the third column in Table I. The dashed line indicates the final result $\kappa_* = 0.00678(6)a_0^{-1}$, as obtained from a weighted average of the four data points of the low-temperature data set (set A; blue squares), and the gray-shaded region shows the corresponding uncertainty. The high-temperature data set (set B; red circles) is not used to derive the final value, but within the uncertainties the values are fully consistent with the result from data set A.

strategies applied. Here the final result for the 3BP, $\kappa_* = 0.00674(13)a_0^{-1}$, is fully consistent with the result obtained at lower temperatures, with an uncertainty about two times larger than that for set A. This confirms that temperature-induced shifts of the resonance are properly taken into account in our theoretical approach.

The original data analysis in Ref. [16] yielded $\kappa_* = 0.0069(2)a_0^{-1}$, which is remarkably close to the present result but had a quoted error about three times larger. However, the present work reveals two systematic shifts which in the previous work partially canceled each other. The updated values of the scattering lengths [48] shift the value of κ_* up by about 3%, while residual finite-temperature effects shift the value down by about 5% [59].

A further contribution to our error budget comes from the uncertainty in the mapping from magnetic field to scattering length. The scattering lengths used here were obtained from the potential curves of Ref. [48], which were fitted to highly precise measurements of binding energies of ^{6}Li$_2$ in the resonant region, together with measurements of collision properties. The fits have recently been extended to include binding energies for ^{7}Li$_2$, with an explicit mass dependence of the potential curves [60]. In order to establish the uncertainties in the scattering lengths at the magnetic field of the excited-state resonance, we have repeated the fits of Ref. [48] and have calculated explicit statistical uncertainties in the scattering lengths a_{12}, a_{13}, and a_{23} at 891 G, using the procedure of Ref. [61]. The resulting contribution to the uncertainty in κ_* is about 0.1%. We have also estimated the nonstatistical uncertainties in the scattering lengths by repeating the fits with the experimental binding energies set to the values at the upper and lower limits of their systematic errors, producing a further uncertainty of 0.07%. The uncertainty of 0.1 G in the magnetic-field calibration of Ref. [16] corresponds to a further error of 0.07%. All these error sources are thus negligibly small compared to the fitting errors described above.

Based on the results of our fits for κ_* and η_*, we can calculate the recombination rate coefficient L_3 in the zero-temperature limit. The resulting curve is shown as a dashed line in Fig. 1. The peak occurs at 891 G, which marks the point where the Efimov state crosses the three-atom threshold. Here the three scattering lengths are $a_{12} = -8671(38)a_0$, $a_{13} = -2866(3)a_0$, and $a_{23} = -5728(16)a_0$.

VI. GROUND-STATE EFIMOV RESONANCES

References [14,15] reported the observation of the two ground-state Efimov resonances in the low-field region of ^{6}Li near 130 G and near 500 G. The L_3 results of Ref. [14] have been further analyzed in Refs. [39,45,46] using different models within the zero-temperature approximation. Reference [46] treated the three different scattering lengths within the approach of the generalized STM equations, which is exact within the zero-range limit, while Ref. [45] introduced the approximation of an "effective scattering length." As an important improvement, Ref. [45] introduced a magnetic-field dependence in the decay parameter η_*, determined by the binding energies of the different target molecular states. The latter has proved very useful to describe the different widths

of the narrower Efimov resonance near 130 G and the wider Efimov resonance near 500 G. Reference [39] considered the effects of finite-range corrections and of a two-channel model of the atom-atom scattering.

Our new analysis of the results of Ref. [14] is based on the generalized STM approach in combination with the magnetic-field-dependent decay parameter η_*. We also use the updated scattering length values from Ref. [48], instead of the ones from Ref. [49], but this has negligible effect on the value resulting for the 3BP in the low-field region. All our fits assume a temperature of 215 nK [14], but we find that including finite-temperature effects makes a negligible difference for the ground-state resonances, in contrast to the excited-state case.

Our theoretical model to calculate L_3 from the three different scattering lengths relies on the zero-range approximation and is applicable only for $|a_{12}|,|a_{13}|,|a_{23}| \gg r_{vdW}$. However, at the resonance positions of 130 and 500 G, the smallest of the three scattering lengths, $|a_{12}|$, exhibits rather small values of $\sim 4r_{vdW}$ and $\sim 3r_{vdW}$, respectively. This makes the analysis quite vulnerable to finite-range effects, and the extracted values for κ_* can be expected to provide only an approximation to the limiting case of Eq. (4). To deal with this nonideal situation, we introduce a lower cutoff scattering length a_{min} and restrict our fit to the region where $|a_{12}|,|a_{13}|,|a_{23}| > a_{min}$. The dependence of the resulting values for κ_* on a_{min} then gives an indication of the sensitivity to finite-range and model-dependent corrections.

Figure 3 shows three different fits to the same data points, differing in the cutoff scattering length, $a_{min}/r_{vdW} = 2, 4$, and 6. The fits are applied globally to both resonances, which appear near 130 G and near 500 G. The three free parameters of the fit are κ_*, the amplitude scaling factor λ (see Sec. V), and the parameter A defined in Ref. [45], from which the magnetic-field-dependent η_* can be calculated. The lines in Fig. 3 represent the behavior within the fit region (solid lines) and extrapolated beyond that region (dashed lines). We find that the fit with $a_{min}/r_{vdW} = 4$ captures both resonances and the overall behavior quite well. Here we obtain $\kappa_* = 0.00645(3)a_0^{-1}$ (linear scale) and $0.00641(3)a_0^{-1}$ (logarithmic scale). For the amplitude scaling factor the fits yield the plausible values $\lambda = 1.65(5)$ (linear) and $1.68(7)$ (logarithmic). From the corresponding values of A we obtain the values $\eta_* = 0.0814(3)$ (linear) and $0.0745(3)$ (logarithmic) for the decay parameter at the lower-field (sharper) resonance, which the fit locates at 132 G.

In contrast to the fit with $a_{min}/r_{vdW} = 4$, the two other fits in Fig. 3 are problematic. The fit for $a_{min}/r_{vdW} = 2$ puts some weight on regions where the applicability of zero-range theory is highly questionable, while the fit for $a_{min}/r_{vdW} = 6$ excludes the centers of the two resonances, which provide the most sensitive information on the Efimov resonance positions.

Figure 4 shows the values for κ_* resulting from fits with different cutoff scattering lengths a_{min} in the range between $2r_{vdW}$ and $6r_{vdW}$. The blue squares represent the fit to the L_3 results on a linear scale. This fit puts the most weight on the lower resonance, but as a_{min} increases, it gives more weight to the region between the resonances, and the resulting value for κ_* decreases by almost 10%. The fits to the L_3 data on a logarithmic scale (red circles) show a similar behavior, with a trend towards smaller values of κ_* at larger values of a_{min}.
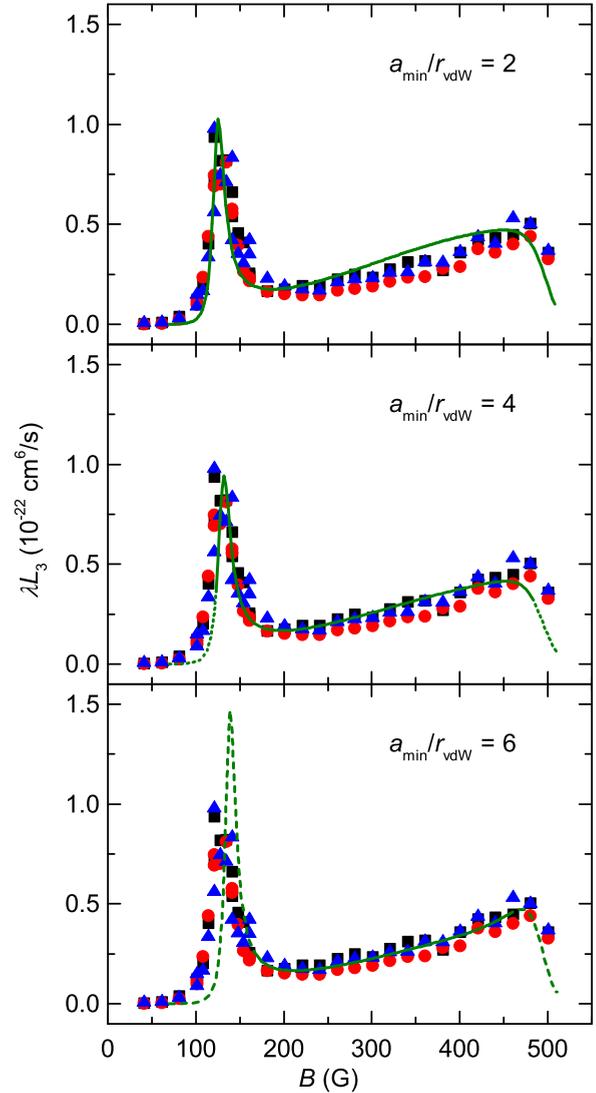

FIG. 3. (Color online) Fits to the ground-state Efimov resonances. All three panels show the same experimental data on the loss rate coefficient L_3 from Ref. [14], where the squares, circles, and triangles refer to losses measured in the lowest three spin states. The theoretical curves represent our fits to the data on a linear scale. The solid lines indicate the region used for the fit in which all three scattering lengths are larger than the cutoff value a_{min}. The dashed lines extrapolate the theory to regions not used for the fit.

The fits for $a_{min}/r_{vdW} \geqslant 5$ do not provide satisfactory results, mainly because of significant problems in reproducing the position of the resonance near 130 G. The fits for $a_{min}/r_{vdW} \leqslant 4$ (middle panel in Fig. 3) appear to be good, but for lower values of a_{min} the result may be subject to significant finite-range effects. We therefore consider $a_{min}/r_{vdW} = 4$ to be the best choice. It gives $\kappa_* = 0.00643(4)a_0^{-1}$, based on averaging the results of the linear and logarithmic fits. The error given here indicates only the statistical uncertainty, but the dependence of the results on a_{min} suggests additional systematic errors on the order of 10%.

The dashed horizontal line and the gray-shaded region in Fig. 4 indicate the value of κ_* obtained from the excited-state resonance in Sec. V, together with the corresponding
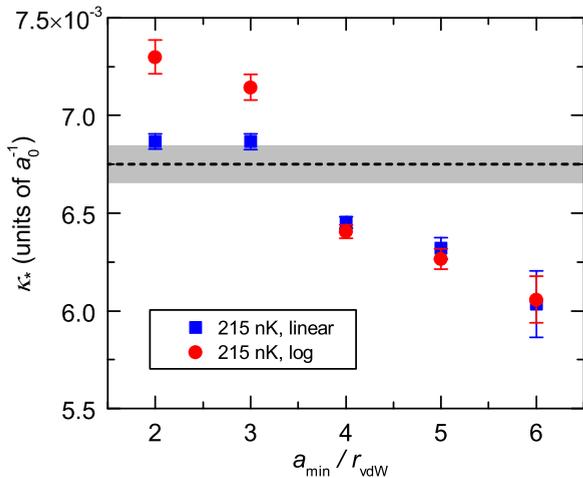
FIG. 4. (Color online) Dependence of the fitted values for κ_* on the cutoff scattering length $a_{\min}$ for the ground-state Efimov resonance. The blue squares and red circles refer to fits performed with linear and logarithmic L_3 scales, respectively. The error bars represent the 1σ uncertainties from the individual fits. The horizontal dashed line marks the value of κ_* obtained from the excited-state Efimov resonance. The gray-shaded region marks the corresponding error range.

error range. It may be seen that our results are consistent with discrete scaling as described by Eq. (1) within the relatively large uncertainties due to finite-range effects in the low-field region.

VII. CONCLUSION

We have reanalyzed experimental results for the Efimov recombination resonances in ^{6}Li arising from the ground and excited Efimov states using a very precise model of the two-body scattering [48] and a new model of temperature-dependent effects in three-body recombinantion of three nonidentical fermions. From the excited-state Efimov resonance [16], we obtain the value for the 3BP in the wave-number representation,

$$\kappa_* = 0.00678(6)a_0^{-1}.$$

This gives the reduced 3BP

$$\kappa_* r_{\mathrm{vdW}} = 0.212(2).$$

According to Eq. (3), this corresponds to a reduced 3BP in the scattering length representation,

$$a_-^* / r_{\mathrm{vdW}} = -7.11(6).$$

This latter representation of the 3BP facilitates a direct comparison with three-boson systems, which are characterized by a single scattering length [62].

Our analysis of the ground-state Efimov resonances [14,15] yields values for the 3BP that are consistent with the above result within an estimated 10% uncertainty. Alternatively, they may be viewed as confirming that the lowest Efimov period in ^{6}Li is within 10% of the universal value of 22.7. The uncertainties, which follow from systematic shifts that depend on the choice of the lower cutoff applied to the scattering lengths in the data analysis, place an upper bound on the magnitude of possible finite-range corrections to the lowest Efimov period. The rapid decrease of such shifts with increasing order of the Efimov state [30,63] gives us confidence that such corrections can be neglected for the 3BP determined from the position of an excited-state resonance.

It is very interesting to compare the present result with the recent measurement for cesium in Ref. [42], which gave $a_-^{(1)} = -20190(1200)a_0$, implying a reduced 3BP $a_-^* / r_{\mathrm{vdW}}^{\mathrm{Cs}} = -8.8(4)$ with $r_{\mathrm{vdW}}^{\mathrm{Cs}} = 101.1a_0$ [43]. In both cases, the Feshbach resonances used for interaction tuning are strongly entrance channel dominated [6]. The present result for the reduced 3BP in ^{6}Li differs from that measured for Cs by a factor of 0.81(4). This clearly demonstrates that the van der Waals length is not the only relevant quantity in determining the 3BP. Even for strongly entrance-channel-dominated Feshbach resonances, van der Waals universality of the 3BP is only approximate and is subject to further influences. It remains a challenge for theory to understand fully the roles of finite-range effects [39], of the physics of particular Feshbach resonances [30,33], of genuine short-range three-body forces [64–66], and of other species-dependent factors such as the number of bound states in the two-body potentials [29]. It is also possible that light particles can tunnel through the barrier in the effective potential [29] more effectively than heavy ones.

It would be highly desirable to investigate other systems at the precision of the present work by detecting excited-state Efimov resonances and thus accurately measuring the 3BP. The bosonic gas of ^{7}Li [9,10,41] is a prime candidate for such experiments because it provides another example of a light system with exceptionally well characterized two-body scattering properties [60,67]. Atoms such as ^{39}K [8,13,68] and ^{85}Rb [12] also provide very interesting systems for future precision experiments: ^{85}Rb offers access to another entrance-channel-dominated case, while ^{7}Li and ^{39}K offer Feshbach resonances of intermediate character [6].

[1] E. Braaten and H.-W. Hammer, Phys. Rep. **428**, 259 (2006).

[2] F. Ferlaino and R. Grimm, Physics **3**, 9 (2010).

[3] V. Efimov, Phys. Lett. B **33**, 563 (1970).

[4] The number 22.7 is rounded to three digits. The relative deviation from the exact value is only 0.025%, which is negligible for all practical purposes.

[5] J. P. D'Incao and B. D. Esry, Phys. Rev. A **73**, 030703(R) (2006).

[6] C. Chin, R. Grimm, P. S. Julienne, and E. Tiesinga, Rev. Mod. Phys. **82**, 1225 (2010).

[7] T. Kraemer, M. Mark, P. Waldburger, J. G. Danzl, C. Chin, B. Engeser, A. D. Lange, K. Pilch, A. Jaakkola, H.-C. Nägerl, and R. Grimm, Nature (London) **440**, 315 (2006).

[8] M. Zaccanti, B. Deissler, C. D'Errico, M. Fattori, M. Jona-Lasinio, S. Müller, G. Roati, M. Inguscio, and G. Modugno, Nat. Phys. **5**, 586 (2009).

[9] S. E. Pollack, D. Dries, and R. G. Hulet, Science **326**, 1683 (2009).

[10] N. Gross, Z. Shotan, S. Kokkelmans, and L. Khaykovich, Phys. Rev. Lett. **103**, 163202 (2009).

[11] N. Gross, Z. Shotan, S. Kokkelmans, and L. Khaykovich, Phys. Rev. Lett **105**, 103203 (2010).

[12] R. J. Wild, P. Makotyn, J. M. Pino, E. A. Cornell, and D. S. Jin, Phys. Rev. Lett. **108**, 145305 (2012).

[13] S. Roy, M. Landini, A. Trenkwalder, G. Semeghini, G. Spagnolli, A. Simoni, M. Fattori, M. Inguscio, and G. Modugno, Phys. Rev. Lett. **111**, 053202 (2013).

[14] T. B. Ottenstein, T. Lompe, M. Kohnen, A. N. Wenz, and S. Jochim, Phys. Rev. Lett. **101**, 203202 (2008).

[15] J. H. Huckans, J. R. Williams, E. L. Hazlett, R. W. Stites, and K. M. O'Hara, Phys. Rev. Lett. **102**, 165302 (2009).

[16] J. R. Williams, E. L. Hazlett, J. H. Huckans, R. W. Stites, Y. Zhang, and K. M. O'Hara, Phys. Rev. Lett. **103**, 130404 (2009).

[17] S. Nakajima, M. Horikoshi, T. Mukaiyama, P. Naidon, and M. Ueda, Phys. Rev. Lett **105**, 023201 (2010).

[18] G. Barontini, C. Weber, F. Rabatti, J. Catani, G. Thalhammer, M. Inguscio, and F. Minardi, Phys. Rev. Lett. **103**, 043201 (2009).

[19] R. S. Bloom, M.-G. Hu, T. D. Cumby, and D. S. Jin, Phys. Rev. Lett. **111**, 105301 (2013).

[20] S.-K. Tung, K. Jimenez-Garcia, J. Johansen, C. V. Parker, and C. Chin, arXiv:1402.5943.

[21] R. Pires, J. Ulmanis, S. Häfner, M. Repp, A. Arias, E. D. Kuhnle, and M. Weidemüller, Phys. Rev. Lett. **112**, 250404 (2014).

[22] H.-W. Hammer and L. Platter, Eur. Phys. J. A **32**, 113 (2007).

[23] J. von Stecher, J. P. D'Incao, and C. H. Greene, Nat. Phys. **5**, 417 (2009).

[24] J. von Stecher, J. Phys. B **43**, 101002 (2010).

[25] F. Ferlaino, S. Knoop, M. Berninger, W. Harm, J. P. D'Incao, H.-C. Nägerl, and R. Grimm, Phys. Rev. Lett. **102**, 140401 (2009).

[26] A. Zenesini, B. Huang, M. Berninger, S. Besler, H.-C. Nägerl, F. Ferlaino, R. Grimm, C. H. Greene, and J. von Stecher, New J. Phys. **15**, 043040 (2013).

[27] M. Berninger, A. Zenesini, B. Huang, W. Harm, H.-C. Nägerl, F. Ferlaino, R. Grimm, P. S. Julienne, and J. M. Hutson, Phys. Rev. Lett. **107**, 120401 (2011).

[28] C. Chin, arXiv:1111.1484.

[29] J. Wang, J. P. D'Incao, B. D. Esry, and C. H. Greene, Phys. Rev. Lett. **108**, 263001 (2012).

[30] R. Schmidt, S. Rath, and W. Zwerger, Eur. Phys. J. B **85**, 386 (2012).

[31] P. K. Sørensen, D. V. Fedorov, A. S. Jensen, and N. T. Zinner, Phys. Rev. A **86**, 052516 (2012).

[32] P. Naidon, S. Endo, and M. Ueda, Phys. Rev. Lett. **112**, 105301 (2014).

[33] Y. Wang and P. S. Julienne, Nat. Phys. **10**, 768 (2014).

[34] B. D. Esry, C. H. Greene, and J. P. Burke, Phys. Rev. Lett. **83**, 1751 (1999).

[35] E. Braaten and H.-W. Hammer, Phys. Rev. Lett. **87**, 160407 (2001).

[36] F. Ferlaino, A. Zenesini, M. Berninger, B. Huang, H.-C. Nägerl, and R. Grimm, Few-Body Syst. **51**, 113 (2011).

[37] M. Thøgersen, D. V. Fedorov, and A. S. Jensen, Europhys. Lett. **83**, 30012 (2008).

[38] L. Platter, C. Ji, and D. R. Phillips, Phys. Rev. A **79**, 022702 (2009).

[39] P. Naidon and M. Ueda, C. R. Phys. **12**, 13 (2011).

[40] J. P. D'Incao, H. Suno, and B. D. Esry, Phys. Rev. Lett. **93**, 123201 (2004).

[41] B. S. Rem, A. T. Grier, I. Ferrier-Barbut, U. Eismann, T. Langen, N. Navon, L. Khaykovich, F. Werner, D. S. Petrov, F. Chevy, and C. Salomon, Phys. Rev. Lett. **110**, 163202 (2013).

[42] B. Huang, L. A. Sidorenkov, R. Grimm, and J. M. Hutson, Phys. Rev. Lett. **112**, 190401 (2014).

[43] M. Berninger, A. Zenesini, B. Huang, W. Harm, H.-C. Nägerl, F. Ferlaino, R. Grimm, P. S. Julienne, and J. M. Hutson, Phys. Rev. A **87**, 032517 (2013).

[44] Z. Zhen and J. Macek, Z. Phys. D **3**, 31 (1986).

[45] A. N. Wenz, T. Lompe, T. B. Ottenstein, F. Serwane, G. Zürn, and S. Jochim, Phys. Rev. A **80**, 040702(R) (2009).

[46] E. Braaten, H.-W. Hammer, D. Kang, and L. Platter, Phys. Rev. Lett. **103**, 073202 (2009).

[47] B. D. Esry, C. H. Greene, and H. Suno, Phys. Rev. A **65**, 010705 (2001).

[48] G. Zürn, T. Lompe, A. N. Wenz, S. Jochim, P. S. Julienne, and J. M. Hutson, Phys. Rev. Lett. **110**, 135301 (2013).

[49] M. Bartenstein, A. Altmeyer, S. Riedl, R. Geursen, S. Jochim, C. Chin, J. Hecker Denschlag, R. Grimm, A. Simoni, E. Tiesinga, C. J. Williams, and P. S. Julienne, Phys. Rev. Lett. **94**, 103201 (2005).

[50] H. A. Bethe, Phys. Rev. **76**, 38 (1949).

[51] O. Hinckelmann and L. Spruch, Phys. Rev. A **3**, 642 (1971).

[52] C. L. Blackley, P. S. Julienne, and J. M. Hutson, Phys. Rev. A **89**, 042701 (2014).

[53] B. Gao, Phys. Rev. A **58**, 4222 (1998).

[54] V. Efimov, Yad. Fiz. **29**, 1058 (1979)[Sov. J. Nucl. Phys. **29**, 546 (1979)].

[55] E. Braaten, H.-W. Hammer, D. Kang, and L. Platter, Phys. Rev. A **78**, 043605 (2008).

[56] D. S. Petrov, in *Proceedings of the Les Houches Summer Schools, Session 94*, edited by C. Salomon, G. V. Shlyapnikov, and L. F. Cugliandolo (Oxford University Press, Oxford, 2013), pp. 109–160.

[57] Fits with both T and λ as free parameters are numerically unstable because the parameters are too strongly correlated.

[58] We use weights that are inversely proportional to the square of the errors of the individual fits. This strongly favors the results obtained from the linear fits (first and third data points in Fig. 2). This is reasonable because these fits are more sensitive to the resonance peaks than the logarithmic fits, which are more sensitive to the wings of the resonance.

[59] In the original analysis, a zero-temperature model was applied to fit only a subset of data in the wings of the resonance, where temperature limitations remain small. This eliminated a large contribution to the temperature-induced shift.

[60] P. S. Julienne and J. M. Hutson, Phys. Rev. A **89**, 052715 (2014).

[61] R. J. Le Roy, J. Mol. Spectrosc. **191**, 223 (1998).

[62] The approximation of an effective scattering length from Ref. [45] leads instead to $a_-^*/r_{vdW} = -8.15(7)$, which is not consistent with our result based on the generalized STM equations. This shows the limited usefulness of the effective scattering length at the precision level of the present work.

[63] M. Thøgersen, D. V. Fedorov, and A. S. Jensen, Phys. Rev. A **78**, 020501(R) (2008).

[64] B. M. Axilrod and E. Teller, J. Chem. Phys. **11**, 299 (1943).

[65] P. Soldán, M. T. Cvitaš, and J. M. Hutson, Phys. Rev. A **67**, 054702 (2003).

[66] J. P. D'Incao, C. H. Greene, and B. D. Esry, J. Phys. B **42**, 044016 (2009).

[67] P. Dyke, S. E. Pollack, and R. G. Hulet, Phys. Rev. A **88**, 023625 (2013).

[68] R. J. Fletcher, A. L. Gaunt, N. Navon, R. P. Smith, and Z. Hadzibabic, Phys. Rev. Lett. **111**, 125303 (2013).